Hyperfine Interact (2013) 221:1–5
DOI 10.1007/s10751-012-0668-6

Observation of transverse spin freezing by TDPAC

T. A. Webb · D. H. Ryan

Published online: 19 October 2012

Abstract We use ^{181}Hf time-differential perturbed angular correlation (TDPAC) spectroscopy to investigate magnetic ordering in the bond-frustrated metallic glass: a $-$ $Fe_{91}Hf_9$. We show that TDPAC can be used to observe the magnetic fluctuations that are associated with the freezing of transverse spin components at T_{xy}.

Keywords TDPAC · Spin glass · Fluctuations · Amorphous · Magnetic ordering · Frustration

1 Introduction

Partial exchange frustration in iron-rich a $-$ Fe_xZr_{100-x} ($90 \leq x \leq 93$) leads to two magnetic transitions: Ferromagnetic order develops at T_C followed by spin glass ordering of transverse spin components at T_{xy} [1]. The behaviour at T_{xy} is masked by the pre-existing and dominant ferromagnetic order, and while applied field techniques can be used, the onset of spin glass order is strongly suppressed by the external field [2, 3], so zero-field methods are preferred. Muon spin relaxation (μSR) revealed signatures of T_C and T_{xy} in both the static and the dynamic behaviour [1]. In particular, the relaxation rate, also observed by selective excitation double Mössbauer spectroscopy (SEDM) [4], exhibits a broad Gaussian peak in fluctuations at T_{xy} and diverges at T_C. Time-differential perturbed $\gamma - \gamma$ angular correlation (TDPAC) spectroscopy, like μSR, is a technique measuring a time-dependent emission anisotropy. In both, simple cases of fluctuating magnetic fields result in an exponential decay of the observed asymmetry [5, 6].

Here we study a $-$ Fe_xHf_{100-x} which exhibits the same magnetic behaviour as the Zr series due to the strong chemical similarity of Hf and Zr [7, 8], and we use this to demonstrate that TDPAC is indeed sensitive to the fluctuations that occur at T_{xy}.

T. A. Webb (✉) · D. H. Ryan
McGill University, 3600 University Street, Montréal, QC, Canada H3A 2T8
e-mail: webbt@physics.mcgill.ca

2 Experimental methods

a – $Fe_{91}Hf_9$ was prepared by arc-melting stoichiometric quantities of Fe (99.9 %) and Hf (99.9 %) under an Ar atmosphere, followed by melt-spinning on a copper wheel with tangential speed 50 m/s in a He atmosphere. Ribbons were confirmed to be amorphous by X-ray diffraction of both sides. ^{57}Fe Mössbauer spectra were collected down to 5 K and also confirmed the absence of crystalline impurities. Below T_C, the spectra were fitted to an asymmetric Gaussian distribution in hyperfine field with a linear correlation between B_{hf} and isomer shift to reproduce the asymmetry in the spectra. Above T_C, they were fitted using a Gaussian distribution of quadrupole splittings, with a linear correlation between the isomer shift and quadrupole splitting.

^{181}Hf activity was introduced via neutron irradiation and TDPAC spectra, using the (133 keV–482 keV) $\gamma - \gamma$ cascade populated by the decay of ^{181}Hf, were then collected on a digital spectrometer [9] with four BaF_2 scintillation detectors in the standard 90°–180° planar geometry. Timing resolution ranged from 350 ps to 500 ps full width at half the maximum among detector pairs on ^{60}Co. Temperatures down to 18 K were reached in a closed cycle He refrigerator.

3 TDPAC data analysis

The TDPAC spectra were calculated from the geometric averages of the eight 90° and four 180° coincidence spectra, $N(180, t)$ and $N(90, t)$, respectively [10]:

$$R(t) = 2\frac{N(180, t) - N(90, t)}{N(180, t) + 2N(90, t)}. \tag{1}$$

Spectra were fitted to $AG_2(t)$. Several modifications to the standard polycrystalline perturbation factor, $G_2^{CR}(t) = \sum_i a_i \cos(\omega_i t)$ [11], were required for these amorphous materials with dynamic internal fields:

$$G_2(t) = \left[a_e e^{-\lambda t} + (1 - a_e)\right] \sum_{i=0}^{3} a_i f(\omega_i, t) \cos(\omega_i t). \tag{2}$$

The exponential factor outside the sum approximates the effect of fluctuations in B_{hf}, playing a role similar to the that of the stretched exponential in early μSR data analysis [12]. The factor $f(\omega_i, t)$ inside the sum consist of two factors modifying the intensities of the oscillatory components: $\exp(-\frac{1}{2}\omega_i^2\tau^2)$ to account for finite time resolution [13] and $\exp(-\frac{1}{2}(2-\alpha)(\delta_i\omega_i t)^{1+\alpha})$ for continuous distributions in the contributing frequencies ω_i. The latter is expected both above and below T_C due to structural and magnetic disorder. The parameter α was introduced to interpolate smoothly between the forms for Gaussian ($\alpha = 1$) and Lorentzian ($\alpha = 0$) distributions [14]. At room temperature where pure EFG are expected and 18 K where a dominant static B_{hf} is expected, α was fixed to 1.0.

A numerical diagonalization of the combined interaction Hamiltonian was used to calculate the a_i and ω_i [11]. The magnetic order is not expected to correlate with the structural order, so a Monte Carlo average over the orientation of B_{hf} with respect to the EFG was performed. To allow for independent distribution widths in the Larmor frequency ω_L and the quadrupole frequency ω_Q ($\delta_B\omega_L$ and $\delta_Q\omega_Q$, respectively), all

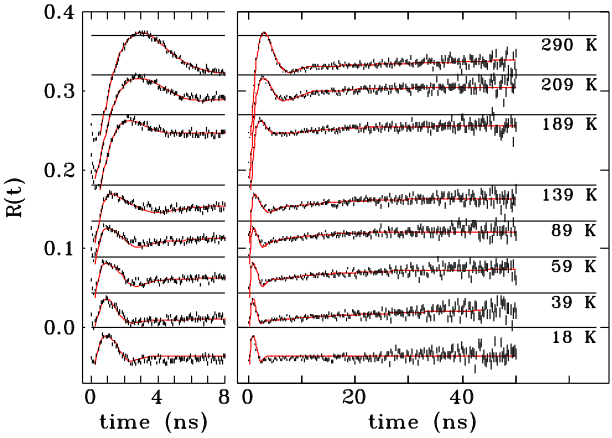

Fig. 1 Representative TDPAC spectra. *Left* and *right* show early and late time behaviour, respectively. *Horizontal lines* indicate the zero of each spectrum

contributing frequencies ω_i were recalculated for small variations in ω_L and ω_Q, and distribution width parameters δ_i were calculated from the two contributions.

Instrument dependent parameters (A, τ and the time origin t_0) were taken from the 18 K spectrum, fitted assuming no dynamics ($\lambda = 0$). The axial asymmetry of the EFG, η, was held fixed to the room temperature value for all spectra. Below 180 K, ω_Q and δ_Q were also fixed to the room temperature values and above 240 K, B_{hf} was set to zero.

4 Results

Representative TDPAC spectra are shown in Fig. 1. The room temperature spectrum gives a distribution in ω_Q centred at 93(1) Mrad/s with η of 0.51(1). The distribution is broad, with a δ_Q of 0.35(1), consistent with the disorder expected in amorphous materials [15]. For this value of η, the average ω_Q gives rise to primary frequency, ω_1, 698 Mrad/s. The 18 K spectrum has a much steeper rise due to higher frequency contributions. The average B_{hf} extracted, 13(1) T, corresponds to Larmor frequency 1.2 Grad/s (Fig. 2). Comparison of ω_L to ω_1 at room temperature indicates that the quadrupole interaction is of comparable strength to the magnetic dipole interaction and cannot be ignored or treated with an approximation. This is in contrast with μSR where the spin-$\frac{1}{2}$ muon is insensitive to the effects of an EFG, and ^{57}Fe Mössbauer spectroscopy where the iron atom carries a large local moment and the resulting B_{hf} is much larger than the EFG.

The average B_{hf} at Hf sites from TDPAC and at Fe sites from Mössbauer spectroscopy (Fig. 2) were fitted to Brillouin functions modified for disorder [16]. The two data sets are in excellent agreement, placing T_C at 195(2) K and 193(1) K, respectively. Below approximately 80 K, B_{hf} has a stronger temperature dependence than the fitted function, expected from the contributions of the ordering transverse spin components [17]. However, the large uncertainties mask the break and prevent extraction of T_{xy}.

At intermediate temperatures, a decay which we attribute to fluctuations in B_{hf} clearly appears in the TDPAC spectra. While similar behaviour could be induced by

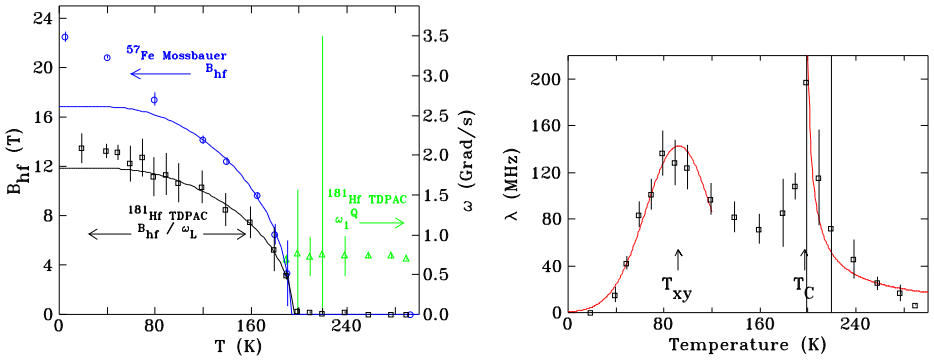

Fig. 2 *Left*: *Circles*: average B_{hf} at Fe nuclei measured by Mössbauer. *Squares*: average B_{hf} (ω_L on right hand scale) at Hf nuclei measured by TDPAC. *Triangles*: average ω_Q from TDPAC, scaled for comparison to ω_L. *Right*: Inverse time constant describing the decay observed in TDPAC spectra. Signatures of both T_{xy} and T_C are visible. *Solid lines* represent fits of the low and high temperature data to a Gaussian and an inverse power law divergence

improper background subtraction prior to R(t) calculation [10], the behaviour does not correspond to the chronological order of acquisition, eliminating the possibility of instrumental drift. The inverse time constant, λ, which describes the decay, peaks at the onset of magnetic order. A broader, smooth peak is observed at lower temperatures, where we expect freezing of the transverse spin degrees of freedom. This close consistency with earlier μSR work on the Zr-based series confirms that the decay is not the result of an instrumental artefact. Unfortunately, we cannot relate λ to an actual relaxation frequency because we are unable to fully account for fluctuations in B_{hf} in the presence of an EFG which is static but differs in strength and orientation among Hf sites. The values for λ that we obtain here are significantly larger than the relaxation frequencies from μSR and SEDM studies of $a-Fe_xZr_{100-x}$. Fitting the low temperature peak in λ to a Gaussian and the high temperature feature to an inverse power law places T_{xy} at 92(2) K and T_C at 197(1) K.

5 Discussion

We have shown that despite the presence of a large static B_{hf} and an EFG of comparable strength, TDPAC is sensitive to the fluctuations at both magnetic transitions in $a-Fe_{91}Hf_9$. The disorder in amorphous materials, causing the heavy damping of oscillations in the spectra, allows the decay of the zero-frequency component to be seen very clearly. However, near T_C, the separation between these two timescales diminishes and distinguishing effects due to the shape of underlying frequency distributions from the effects of dynamics was not possible.

TDPAC is able to play a similar role to μSR in the study of dynamics in bond frustrated materials, showing the same qualitative behaviour of both static and dynamic features. The significant computational complications associated with comparable effects of B_{hf} and the EFG in the current system limits the analysis of the dynamic response in the current system, however this might not be the case in a system where the TDPAC probe was itself magnetic.

Acknowledgements This research was supported by grants from the Natural Sciences and Engineering Research Council of Canada and Fonds Québécois de la Recherche sur la Nature et les Technologies. Neutron activation was carried out by M. Butler at the McMaster Nuclear Reactor (MNR), Hamilton Ontario.

References

1. Ryan, D.H., van Lierop, J., Cadogan, J.M.: J. Phys.: Condens. Matter **16**, S4619 (2004)
2. Ryan, D.H., van Lierop, J., Pumarol, M.E., Roseman, M., Cadogan, J.M.: Phys. Rev. B **63**, 140405 (2001)
3. Beath, A.D., Ryan, D.H., Cadogan, J.M., van Lierop, J.: J. Appl. Phys. **111**, 07E108 (2012)
4. van Lierop, J., Ryan, D.H.: Phys. Rev. Lett. **86**, 4390 (2001)
5. Winkler, H., Gerdau, E.: Z. Phys. **262**, 363 (1973)
6. Uemura, Y.J., Yamazaki, T., Harshman, D.R., Senba, M., Ansaldo, E.J.: Phys. Rev. B **31**, 546 (1985)
7. Ryan, D.H., Coey, J.M.D., Ström-Olsen, J.O.: J. Magn. Magn. Mater. **67**, 148 (1987)
8. Ren, H., Ryan, D.H.: Phys. Rev. B **51**, 15885 (1995)
9. Webb, T.A., Nikkinen, L., Gallego, J., Ryan, D.H.: Hyperfine Interact. (2012). doi:10.1007/s10751-012-0663-y
10. Arends, A.R., Hohenemser, C., Pleiter, F., de Waard, H., Chow, L., Suter, R.M.: Hyperfine Interact. **8**, 191 (1980)
11. Frauenfelder, H., Steffen, R.M.: In: Siegbahn, K. (ed.) Alpha-, Beta- and Gamma-Ray Spectroscopy, p. 997. North-Holland, Amsterdam (1965)
12. Ryan, D.H., Cadogan, J.M., van Lierop, J.: Phys. Rev. B **61**, 6816 (2000)
13. Béraud, R., Berkes, I., Danière, J., Marest, G., Rougny, R.: Nucl. Instrum. Methods **69**, 41 (1969)
14. Rogers, J.D., Vasquez, A.: Nucl. Instrum. Methods **130**, 539 (1975)
15. Czjzek, G., Fink, J., Götz, F., Schmidt, H., Coey, J.M.D., Rebouillat, J.P., Liénard, A.: Phys. Rev. B **23**, 2513 (1981)
16. Handrich, K.: Phys. Stat. Sol. **32**, K55 (1969)
17. Ryan, D.H., van Lierop, J., Pumarol, M.E., Roseman, M., Cadogan, J.M.: J. Appl. Phys. **89**, 7039 (2001)